

Special Issue on Calibration Research in Russia

Articles

CAL/VAL system for Russian satellite instruments

by A. Rublev (State Research Center for Space Hydrometeorology, Roshydromet)

IKFS-2 radiometric calibration stability in different spectral bands

by F. Zavelevich, D. Kozlov, I. Kozlov, I. Cherkashin (State Scientific Center "Keldysh Research Center", Russia), A. Uspensky, Yu. Kiseleva, V. Golomolzin and A. Filei (State Research Center for Space Hydrometeorology "Planeta", Roshydromet)

Assessment and Recalibration of Meteor-M No.2 Microwave Imager/Sounder MTVZA-GY data in Atmospheric Sounding Channels

by D. Gayfulin and M. Tsyrlunikov (Hydrometcenter of Russia) and A. Uspensky (SRCSH, "Planeta", Roshydromet)

External Calibration of MTVZA-GY/ Meteor-M No.2 Imager Channels

by L. Mitnik, V. Kuleshov (Pacific Oceanological Institute), G. Chernyavsky and I. Cherny (AO Russian Space System)

Radiometric inter-calibration of MSU-MR shortwave channels on-board Meteor-M No. 2 relative to AVHRR on-board Metop A

by A. Filei, A. Rublev (State Research Center for Space Hydrometeorology "Planeta", Roshydromet) and A. Zaitsev (Joint Stock Company Russian Space Systems)

Radiometric inter-calibration between MSU-GS and VIIRS shortwave channels

by A. Filei, A. Rublev, Yu. Kiseleva (SRCSH "Planeta", Roshydromet) and A. Zaitsev (Joint Stock Company "Russian Space Systems")

News in This Quarter

Highlights on 2018 Annual GRWG/GDWG Meeting

by M. Bali (UMD), L. Flynn (NOAA), P.Zhang (CMA), S. Hu (CMA), T. Stone (USGS), D. Doelling (NASA), R. Ferraro (NOAA), T. Hewison (EUMETSAT), D. Kim (KMA) and M. Takahashi (JMA)

GOES Calibration Web Site

by R. Iacovazzi, Jr (NOAA)

Announcements

Call for papers for 2nd Workshop of the CGMS International Cloud Working Group (ICWG)

by Andy Heidinger (NOAA) and Rob Roebeling (EUMETSAT)

Sentinel-3B Mission launched

by Tim Hewison and Alessandro Burini (EUMETSAT)

GSICS Related Publications



Image Above shows Roshydromet observation network and test sites

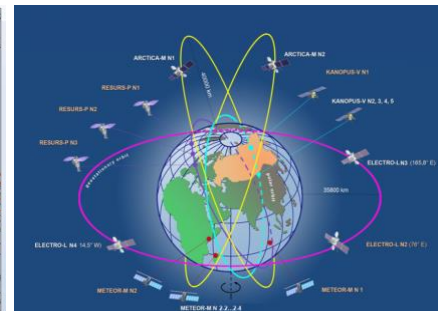


Image Above shows satellites of Russian Earth Observation System

CAL/VAL system for Russian satellite instruments

By A. Rublev (State Research Center for Space Hydrometeorology "Planeta", Roshydromet)

Roshydromet and Roscosmos are developing the constellation of the Russian meteorological satellites (next generation). By 2025, it will consist of four Meteor-M low earth orbit (LEO) satellites, three Electro-L geostationary (GEO) satellites, two highly elliptical orbit (HEO) Arctica satellites, and approximately ten R&D environmental satellites. Thus, there is a strong need for dedicated calibration and validation (CAL/VAL) activities with

respect to satellite hydrometeorological data and Level 2 (L2) products. CAL/VAL of satellite data and products are critical for many applications. To better examine the quality of existing and future developed information products the Cal/Val system for meteorological satellite data was enhanced and implemented in 2016. The system takes as input the data of global and Roshydromet observing networks, results of test site measurements and data of reference satellite instruments recommended by GSICS. The illustrative scheme of the system is presented in Fig.1.

The main tasks of CAL/VAL system are as follows:

- 1) post-launch calibration and characterization of on-orbit calibration performance for current and future Russian LEO, GEO, and HEO meteorological satellite instruments; and
- 2) validation of L2 products, i.e. the assessment of L2 products accuracy and reliability based on comparison with reference data (with known accuracy).

This special issue of GSICS Quarterly Newsletters is dedicated to the use of the

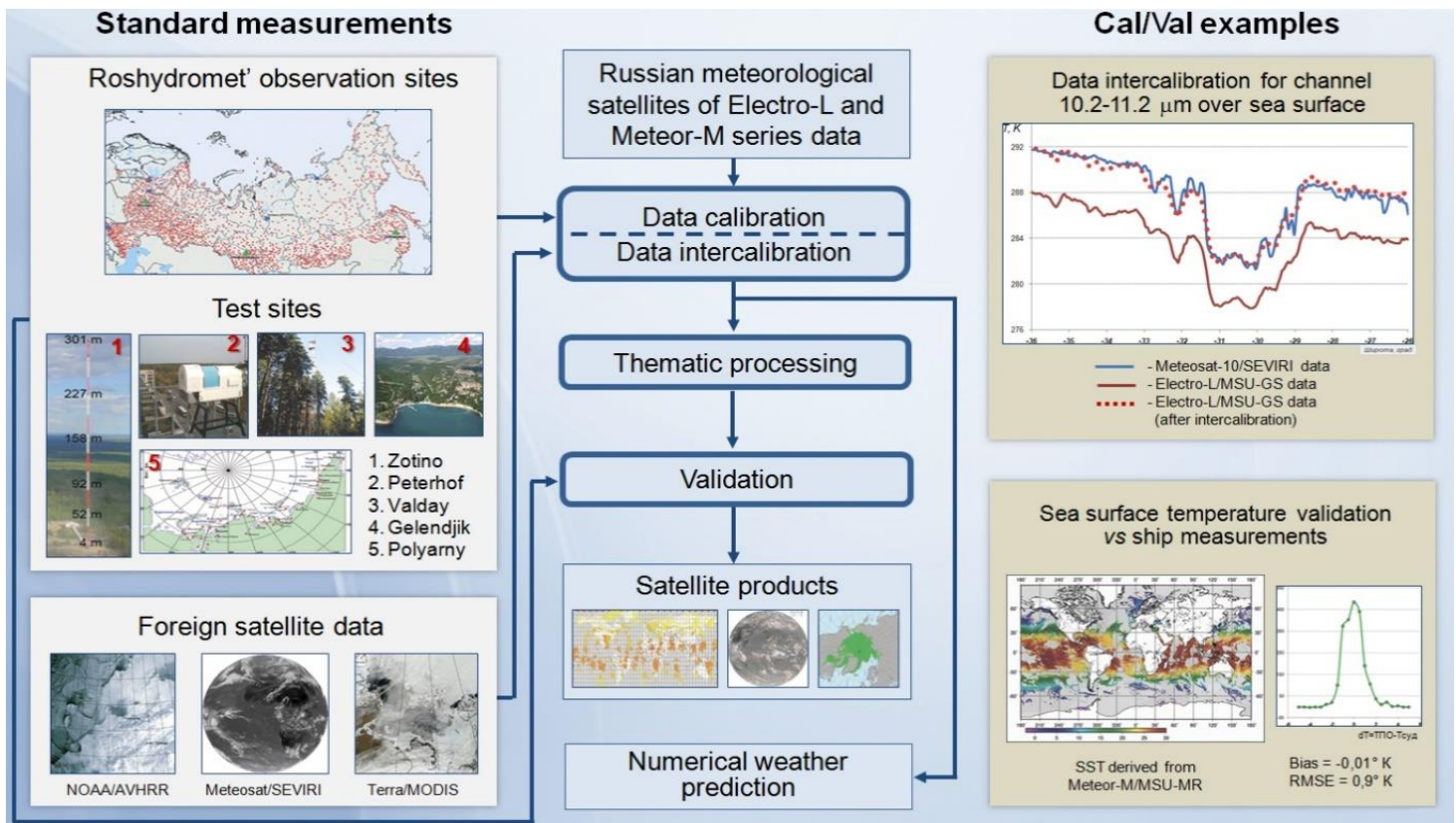


Figure 1. CAL/VAL System for Satellite Data and Products (<http://planet.rssi.ru/calval>)

Cal/Val system for solving the first task. The papers presented here describe the external (including inter-) calibration of radiometers which are part of the payloads of two Russian meteorological satellites – LEO Meteor-M (Meteor-M) No.2 and GEO Electro-L No.2.

A space observation system of new-generation polar-orbit meteorological satellites of the Meteor-M type is now being developed in Russia. In July 2014 one such satellite, Meteor-M N2, was launched in the sun-synchronous orbit with an altitude 830 km and an equator crossing local solar time of $\sim 9:30$ am in descending node. From the present until 2025, four or five Meteor-M type satellites will be launched in both the morning and the afternoon orbits. Their payloads contain, inter alia, two atmospheric sounders: the

IKFS-2 hyperspectral infrared sounder, MTVZA-GY microwave sounder and the MSU-MR imager, analogous to AVHRR (Advanced Very High Resolution Radiometer).

In the paper of Zavelevich et al., 2018, the authors presented results of intercalibration of IKFS-2 on Meteor-M No.2 satellite using IR channels of SEVIRI/Meteosat-10 and the interferometer IASI/Metop-A(B) as reference instruments. The IKFS-2 intercalibrations, which were carried out during 2015-2018, indicate the proper quality and stability of its radiometric and spectral characteristics. The successful functioning of IKFS-2 allowed development and testing of the operational IKFS-2 L2 processor to retrieve target geophysical parameters including atmospheric temperature and humidity profiles

(http://planet.iitp.ru/Oper_pr/ikfs-2/index.php?lang=en). The CO_2 column-averaged mixing ratio maps for Central Siberia and the Pacific Ocean have been constructed from the beginning of 2018 to the present (<http://www.rcpod.ru>). The RMS error of the satellite estimates under clear sky conditions does not exceed 1.5 ppm. Two papers consider the external calibration of the second sounder on board Meteor-M No.2 - the microwave radiometer MTVZA-GY with imaging/sounding functions (unfortunately, starting from August 2017, this instrument is no longer operational). MTVZA-GY data undergo an on-orbit radiometric calibration: a two-point calibration technique converts the electric signal to the antenna brightness temperature T_a . Soon after launch, large global and

air mass dependent biases in antenna temperatures along with ascending-descending bias differences were found by comparing the observed T_a with the reference (simulated) brightness temperatures T_b .

To reduce biases, related to calibration issues, two post-launch calibration or recalibration algorithms were developed and implemented for MTVZA-GY atmospheric sounding channels. At first, a recalibration algorithm was proposed based on the linear regression between observed T_a 's and reference T_b 's. Later, to further improve MTVZA-GY data quality, a more advanced recalibration technique was proposed, in which the coefficients in linear regression are assumed to be functions of the solar azimuth and zenith angles, available for each pixel. Both recalibration techniques are outlined in the paper of Gayfulin et al. (2018).

Mitnik and coauthors (2018) consider questions of external calibration of MTVZA-GY imager channels. Hot references areas were selected in the broadleaf rainforests of the Amazon. The cases with heavy clouds and rains were removed using the measurements at frequencies $\nu \geq 36\text{GHz}$. The joint analysis of T_b 's at $\nu = 10.6$ and 42.0 GHz with horizontal polarization allowed us to find the cold cloudless references areas around Antarctica. The T_b 's of the test areas were computed using the known daily values of the forest emissivity, SST and atmospheric water vapor content retrieved by other satellite sensors. The high stability of MTVZA-GY in flight was shown by comparison of the T_b 's time series (October 2014 - July 2017) obtained for

test areas by MTVZA-GY and GCOM-W1 AMSR2 at coinciding frequencies. SRC "Planeta" began to provide intercalibration of MSU-MR/Meteor-M No.2 and MSU-GS/Electro-L No.2 shortwave channels two years ago. The aims of this activity are to develop novel techniques suitable for assessing macro – and microphysical parameters of water and ice clouds as well as volcanic ash and desert dust aerosols. Two papers presented by Filei and et al. (2018 a, b) contain the results of intercalibration for shortwave channels of both imagers.

In the first paper, Filei and et al. (2018 a) present the results of radiometric inter-calibration of MSU-MR shortwave channels versus radiometer AVHRR /Metop-A. The intercalibration of MSU-MR implies a comparison of the reflectance at the top of atmosphere (TOA) of two instruments above six desert sites proposed by CEOS (Committee on Earth Observation Satellites). The conditions of observations are very close: small (less than 2°) discrepancies in observation angles and positions of the Sun; the time intervals between measurements of the two instruments are not more 15 minutes. More than 2000 matched TOA reflectance pairs were used for each site. After performing the inter-calibration, it is possible to merge the AVHRR & MSU-MR data to calculate various complex indices characterizing the state of the underlying surface.

The second paper (Filei and et al. 2018 b) is devoted to GEO- LEO intercalibration of MSU-GS imager on board of Electro-L No.2. The Russian Electro-L No.2 satellite was launched on December 11, 2015 and positioned

at 76° east longitude. In general, the MSU-GS images from shortwave channels are very similar in quality to those from SEVIRI onboard Meteosat satellites. The VIIRS (Visible Infrared Imaging Radiometer Suite) onboard the LEO Suomi NPP (Suomi National Polar-Orbiting Partnership) was selected as a reference instrument. VIIRS was used as a reference because it regularly participates in intercalibrations and has channel spectral response functions similar to MSU-GS. For intercalibration, the authors use the comparison of reflectance at the TOA measured by both instruments above deep convective clouds (DCCs) over the Indian Ocean for six months of 2017. The difference in calibration amounts is 12% but the long term stability of calibration coefficients is better than 1%. The DCC technique is an alternative variant of the target calibration approach used for MSU-MR/Meteor-M No.2 and described in the previous paper. The papers presented in this issue describe only some applications of Russian Cal/Val system for external calibration of Russian meteorological satellite instruments. You can find other materials in a special dedicated site: <http://planet.rssi.ru/calval>.

References

Filei, A., Rublev, A., Zaitsev, A., 2018a, Radiometric inter-calibration of MSU-MR shortwave channels on-board Meteor-M No. 2 relative to AVHRR on-board Metop-A. In this issue, GSICS Quarterly Newsletter.

Filei, A., Rublev, A., Kiseleva, Yu., 2018b, Radiometric inter-calibration between MSU-GS and VIIRS shortwave channels. In this issue, GSICS Quarterly

Newsletter.

Gayfulin, D., Tsyulnikov, M., Uspensky, A., 2018, Assessment and recalibration of Meteor-M No. 2 microwave imager/sounder MTVZA-GY data in atmospheric sounding channels. In this

issue, GSICS Quarterly Newsletter.

Mitnik, L., Kuleshov, V., Chernyavsky, G., Cherny, I. 2018, External Calibration of MTVZA-GY/Meteor-M No.2 imager channels. In this issue, GSICS Quarterly Newsletter.

Zavelevich, F., Kozlov, D., Kozlov, I., Cherkashin, I., Uspensky, A., Kiseleva, Yu., Golomolzin, V., Filei, A., 2018, IKFS-2 radiometric calibration stability in different spectral bands. In this issue, GSICS Quarterly Newsletter.

[Discuss the article](#)

IKFS-2 radiometric calibration stability in different spectral bands

by F. Zavelevich, D. Kozlov, I. Kozlov, I. Cherkashin (State Scientific Center “Keldysh Research Center”, Russia),

A. Uspensky, Yu. Kiseleva, V. Golomolzin and A. Filei (State Research Center for Space Hydrometeorology “Planeta”, Roshydromet)

The infrared Fourier transform spectrometer, IKFS-2, is a part of the Meteor-M2 operational meteorological satellite and provides well calibrated hyperspectral data (atmospheric emission spectra) for weather prediction and climate studies. The instrument is based on Michelson interferometer with a double pendulum optical path difference (OPD) scan mechanism, cross-track scanning device and two stage passive radiant cooler to provide cooling of the MCT (HgCdTe) photoconductive detector (Golovin et al., 2014). The main technical characteristics of IKFS-2 are presented in Table 1.

The IKFS-2 instrument status and data quality have been comprehensively investigated during the commissioning phase and exploitation. More detailed analysis of the spectra measured by IKFS-2 instrument is presented in (Polyakov et al., 2017).

Intercomparisons of IKFS-2 data with collocated IASI and CrIS spectra show that the discrepancies in the average spectra and their variability do not exceed the measurement noise.

To monitor and control the IKFS-2 radiometric and spectral calibration accuracy and stability, intercalibration

with independent satellite measurements is needed. In this article, the results of IKFS-2 intercomparison with SEVIRI and IASI measurements are presented obtained for three years of continuous monitoring.

The procedure used for SEVIRI and IKFS-2 intercomparison is almost fully identical to one used for SEVIRI and IASI (EUMETSAT, 2016). The collocation criteria are based on those recommended by GSICS:

- the time differences between observations to be less than the Meteosat repeat cycle (15 min);
- the surface incidence angles for IKFS-2 to be no more than 15° from zenith;

- the surface incidence angles for both instruments to be within ~5°;
- both day-time and night-time data are used;
- azimuth angles are not considered. SEVIRI channels 5-11 centered at 6.2, 7.3, 8.7, 9.7, 10.8, 12.0, 13.4 μm are used. The radiance spectrum measured by IKFS-2 is convolved with Spectral Response Function (SRF) of each SEVIRI channel. SEVIRI pixels' radiances are averaged within the effective IKFS-2 field of view area. Effective radiance to brightness temperature (BT) conversions are performed by using an approximation formula with three regression

Table 1. IKFS-2 technical characteristics

Spectral range	660-2000 cm ⁻¹
Spectral resolution (non-apodized)	0.4 cm ⁻¹
Radiometric calibration error	< 0.5 K
Radiometric noise (NESR)	0.15-0.3 mW·cm/(m ² ·sr)
Instantaneous field of view IFOV diameter at SSP	40 mrad 30 km
Swath width Spatial sampling	1000-2500 km 60-110 km
IFG period (sweep + reverse time)	0.6 s
Data rate	600 kb/s
Mass	50 kg
Power	50 W

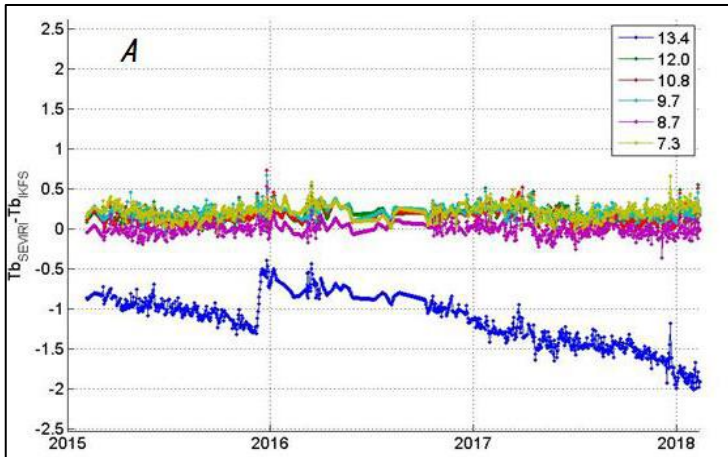


Figure 1. A. SEVIRI/MSG3 and IKFS-2/Meteor-M2 bias monitoring (1-day averaged);

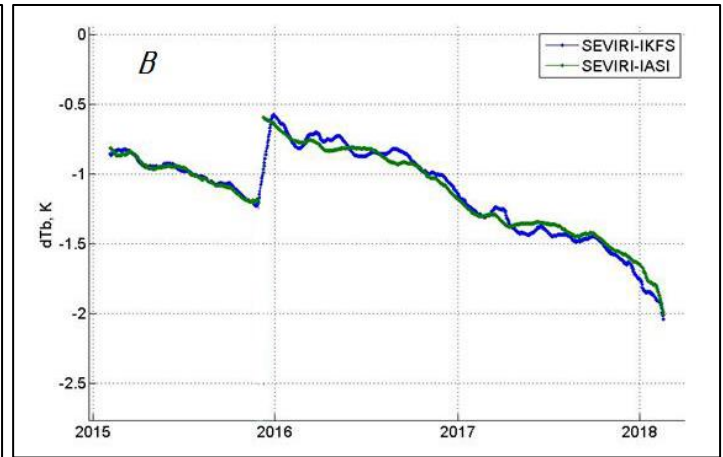


Figure 1. B. SEVIRI-IASI and SEVIRI-IKFS bias time series (13.4 μm channel)

parameters α , β , ν (EUMETSAT, 2012). Additional data filtering to meet more stringent collocation criteria can be applied.

Preliminary results of SEVIRI and IKFS-2 intercalibration were presented in (Kozlov et al., 2016). Firstly, it was shown that (SEVIRI-IKFS) BT differences for all channels are less than 0.3 K with the exception of channels centered at 6.2 and 13.4 μm . Secondly a well-known problem with the IR13.4 SEVIRI channel calibration due to ice contamination was observed leading to ~ 1 K BT difference.

Thirdly, there are some problems with IKFS-2 calibration in the shortwave region (WV6.2 channel) caused by residual nonlinearity correction errors. The results of SEVIRI and IKFS-2 intercomparison are summarized over three years. SEVIRI/MSG-3 and IKFS-2/Meteor-M2 bias monitoring is shown in Figure 1A (from Feb 2015 to Feb 2018). All channels except from IR13.4 are consistent within ~ 0.3 K. Moreover, BT differences in 13.4 μm channel are changing in time almost identical to SEVIRI-IASI results (Figure 1B).

Using intercalibration data of SEVIRI and IASI available on GSICS portal,

there is a possibility to organize the “double difference” method of IKFS-2 (monitored instrument) and IASI (reference instrument) intercomparison with SEVIRI used as intermediary (transfer) instrument.

In conclusion, the results of direct intercomparison of IKFS-2 and IASI spectrometers are briefly presented. Orbital elements of MetOp and Meteor-M2 satellites are similar providing good conditions for intercomparison. Data from Jan 2015 to Jun 2017 were used from both MetOp-A/IASI and

MetOp-B/IASI. As usual, the time, spatial and geometrical mismatches are taken into account in collocation criteria. IASI spectra are converted to IKFS-2 spectral data taking into account differences in OPD range, apodization and spectral grid. Four IASI subpixels spectra (IFOV = 12 km) are averaged to be compared with one IKFS-2 spectrum (IFOV = 30 km).

The standard deviations of the four IASI subpixels spectra are calculated to

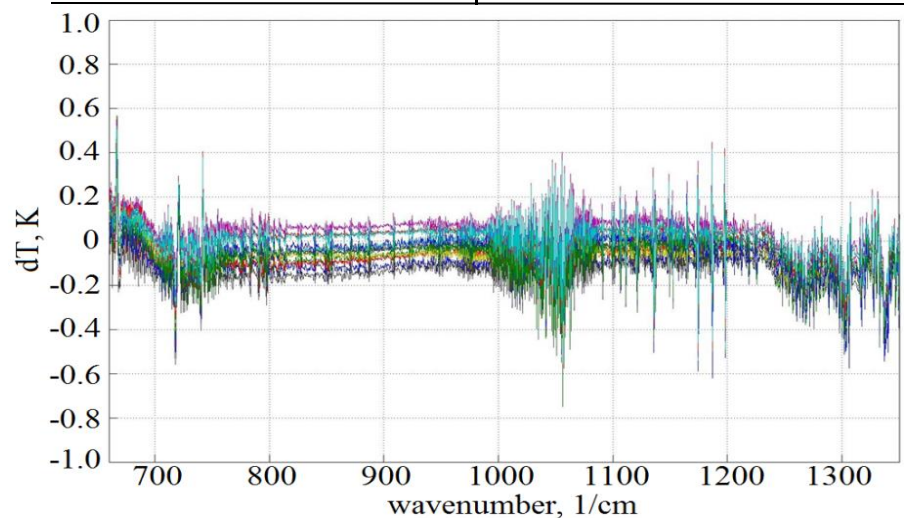


Figure 2: Daily averaged (IKFS-IASI) BT differences from Jul 2015 to Jun 2017 (once per 2 months)

select spatially uniform scenes. Daily averaged BT differences between IASI and IKFS-2 measurements are shown in Figure 2. These results, firstly, confirm the proper quality and stability of the radiometric calibration of the IKFS-2 measurements, and secondly, demonstrate the good quality of the spectral calibration of the IKFS-2 instrument. Also, some effect of IKFS-2 instrument line shape characterization error can be seen manifested itself in small spikes in absorption lines. The results presented above confirm the proper quality and stability of the IKFS-2 radiometric calibration.

References:

EUMETSAT, ATBD for EUMETSAT Operational GSICS Inter-Calibration of Meteosat-IASI, EUM/TSS/TEN/15/803179, 2016.

EUMETSAT, The Conversion from Effective Radiances to Equivalent Brightness Temperatures, EUM/MET/TEN/11/0569, 2012.

Golovin, Yu. et al., Spaceborne infrared Fourier transform spectrometers for temperature and humidity sounding of the Earth's atmosphere, *Izv. Atmos. Ocean. Phys.*, 2014, Vol. 50, No. 9, 1004–1015,

10.1134/S0001433814090096. Kozlov, D. A. et al., IRFS-2 onboard radiometric calibration errors evaluation by comparison with SEVIRI/Meteosat-10 data, *Sovremennye problemy distantsionnogo zondirovaniya Zemli iz kosmosa*, 2016, Vol. 13, No. 6, 264–272, 10.21046/2070-7401-2016-13-6-264-272.

Polyakov, A.V. et al., Satellite atmospheric sounder IRFS-2. Analysis of outgoing radiation spectra measurements, *Izv. Atmos. Ocean. Phys.*, 2017, Vol. 53, No. 9, 1185–1191, 10.1134/S0001433817090249.

[Discuss the article](#)

Assessment and Recalibration of Meteor-M No. 2 Microwave Imager/Sounder MTVZA-GY data in Atmospheric Sounding Channels

by D. Gayfulin, M. Tsyrlunikov (Hydrometcenter of Russia) and A. Uspensky (State Research Center for Space Hydrometeorology "Planeta", Roshydromet)

One of the key instruments onboard Russian polar-orbiting meteorological satellites of the Meteor-M type is the microwave imager/sounder MTVZA-GY. In this study, the performance of MTVZA-GY onboard Meteor-M No. 2 (launched in July, 2014) has been examined (note that starting from August 2017, this instrument is no longer operational). From the present until 2025, four or five Meteor-M type satellites will be launched in both the morning and the afternoon orbits, with the first launch in late 2018. Data

produced by MTVZA-GY will be available to direct readout users. The MTVZA-GY instrument is a passive microwave radiometer with 29 channels in the 10.6–183.3 GHz frequency range and a conical scanning regime. The viewing angle is 53.3° and the incidence angle with respect to the Earth surface is 65°. A two-point on-board calibration technique is used for converting measured signals to antenna brightness temperatures T_a (Cherny et al., 2010).

An initial assessment of the MTVZA-

GY data in atmospheric sounding channels was performed in (Uspensky et al., 2015). Large global and air-mass dependent biases were found by comparing the observed T_a with the *reference* (simulated) T_b , see Row 1 in Table 1 below. The *reference* brightness temperatures were computed by using a fast radiative transfer model similar to the well-known RTTOV or specifically RTTOV v.11 (Hocking et al., 2014). NCEP analyses were used as input to the radiative transfer model.

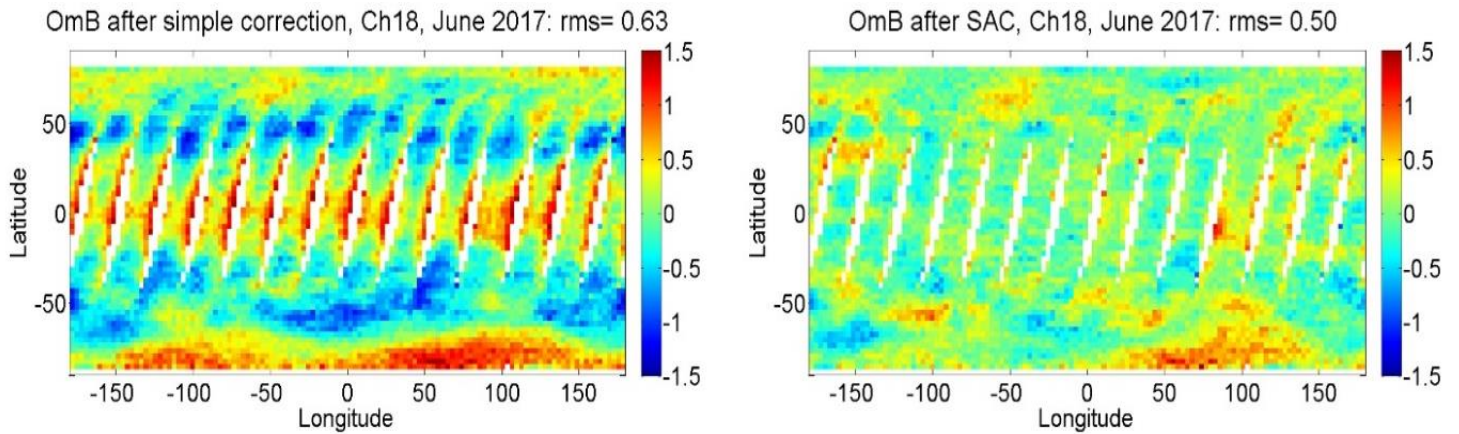


Figure 1: Local biases for observations in channel 18 at times from 21h UTC, 12 June 2017 to 3h UTC, 14 June 2017 (descending orbits). *Left:* With the “simple” recalibration scheme. *Right:* With the SAC scheme.

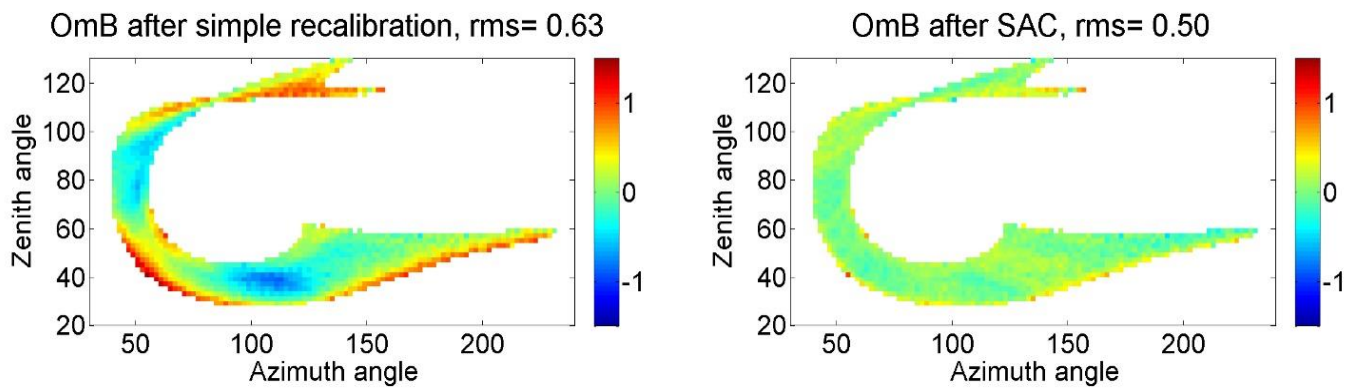


Figure 2: Same as Fig.1 but on the α - ζ plane.

To mitigate possible calibration issues, a recalibration technique (called the “simple” recalibration in the following) was developed and implemented for MTVZA-GY atmospheric sounding channels (Uspensky et al., 2015; Uspensky et al.2017). The technique is based on the linear regression

$$T_b = a T_a + b, \quad (1)$$

where T_a is the raw antenna temperature, T_b is the recalibrated brightness temperature, and a and b are the regression coefficients (estimated from a training sample of the observed T_a 's and collocated reference T_b 's). Recalibrated and bias-corrected MTVZA-GY data were then assimilated into the global data

assimilation system of the Hydrometcenter of Russia (Gayfulin et al.,2017). A significantly positive impact of MTVZA-GY observations in the Southern Hemisphere was found in the absence of AMSU-A observations. To further improve MTVZA-GY data, a new recalibration/correction technique was proposed in (Gayfulin et al., 2017), in which the calibration coefficients a and b in Eq. (1) are assumed to be functions of the solar azimuth and zenith angles α and ζ . In this technique (called SAC – Solar-Angles reCalibration) the gridded fields $\mathbf{a}(\alpha;\zeta)$ and $\mathbf{b}(\alpha;\zeta)$ (represented by the vectors $\vec{\mathbf{a}}$ and $\vec{\mathbf{b}}$) are cyclically updated

every 6 hours in a variational scheme, which aims to minimize the cost function

$$J(\vec{\mathbf{a}}, \vec{\mathbf{b}}) = J_{obs}(\vec{\mathbf{a}}, \vec{\mathbf{b}}) + J_{fg}(\vec{\mathbf{a}}, \vec{\mathbf{b}}) + J_{smo}(\vec{\mathbf{a}}, \vec{\mathbf{b}}) \rightarrow \min, \quad (2)$$

where the J_{obs} term penalizes deviations of observations (T_a) from the reference, $J_{fg}(\vec{\mathbf{a}}, \vec{\mathbf{b}})$ regularizes the problem and allows assimilation of past data by controlling deviations from a first guess (persistence forecast of $\vec{\mathbf{a}}$ and $\vec{\mathbf{b}}$ from the previous cycle), and $J_{smo}(\vec{\mathbf{a}}, \vec{\mathbf{b}})$ further regularizes the problem by imposing a smoothness constraint on the fields $\vec{\mathbf{a}}$ and $\vec{\mathbf{b}}$. See (Gayfulin et al., 2018) for more details.

Table 1: RMS errors of raw and recalibrated observations. in K.

Scheme	Ch15	Ch16	Ch17	Ch18	Ch19	Ch20	Ch27	Ch28	Ch29
Raw data	7.53	13.3	15.4	13.5	6.65	10.5	18.4	18.5	13.8
“Simple”	0.67	0.83	1.70	0.62	0.71	0.79	2.00	2.15	2.65
SAC	0.56	0.63	1.04	0.50	0.56	0.62	1.91	2.01	2.38

Figure 1 shows the geographic distributions of local biases (computed by averaging observation-minus-background deviations over $3^\circ \times 3^\circ$ grid cells of the regular grid on the globe) for channel 18 for the 30h period indicated in the figure caption. Comparing the two panels in Fig.1 (the “simple” and the SAC schemes) demonstrates how successfully the developed SAC scheme removes the local biases, leaving behind, primarily, just noise. This conclusion can also be drawn from Fig. 2, which shows the distributions of local biases of recalibrated observations on the α - ζ plane.

RMS errors for raw and recalibrated observations are presented in Table 1 (averaged over three two-week periods in 2017). One can see the very large RMS errors (caused by large biases, not shown) for raw observations and the significant improvements due to both the “simple” and the SAC schemes. Note that channels 15-20 are temperature sounding channels with center frequencies at 52.8, 53.3, 53.8, 54.64, 55.63, 57.29 \pm 0.32 \pm 0.1GHz, while 27-29 are humidity sounding channels with center frequencies at 183.31 \pm 7.0, 183.31 \pm 3.0, 183.31 \pm 1.0

GHz.

It is worth mentioning that after the SAC recalibration, the MTVZA-GY channel 15 appears to be comparable in accuracy to AMSU-A channel 4 (not shown), whereas MTVZA-GY channel 17 exhibits the poorest performance. The RMS errors in the other MTVZA-GY channels were about 1.5-2 times as large as the RMS errors in the similar AMSU-A/MHS channels.

To summarize, a new recalibration / correction algorithm for MTVZA-GY atmospheric sounding channels has been proposed. The technique sequentially assimilates observed minus simulated radiance data in a 6h cycle in order to estimate up-to-date calibration coefficients. The calibration coefficients are defined to be functions of the solar azimuth and zenith angles. The solar-angles dependent recalibration technique is shown to produce significantly more accurate data as compared with raw observations and with observations that undergo a simpler recalibration technique.

References

Cherny, I., Mitnik, L., Mitnik, M. 2010. On-orbit calibration of the Meteor-M microwave imager/sounder.

In Geosci. Rem. Sens. Symp. (IGARSS), IEEE, 558–561

Gayfulin, D., Tsyrlunikov M., Uspensky A. 2017. The usage of MTVZA-GY a satellite microwave radiometer observations in the data assimilation system of the Hydrometcenter of Russia. Russ. Meteorol. Hydrol., Vol.42, No. 9, 564-573.

Gayfulin, D., Tsyrlunikov M., Uspensky A. 2018. Assessment and Adaptive Correction of Observations in Atmospheric Sounding Channels of the Satellite Microwave Radiometer MTVZA-GY. Pure and Applied Geophysics (in press), DOI: 10.1007/s00024-018-1917-7.

Hocking, J., Rayer, P.J., Rundle, D., Saunders, R.W., Matricardi, M., Geer, A., Brunel, P. and. Vidot, J. 2014. RTTOV v11 Users Guide; NWP-SAF Report NWPSAF-MO-UD-028

Uspensky, S., Kramchaninova, E., Uspensky, A., Poli, P., English, S., Lupu, C. 2015. An initial assessment of microwave imager/sounder MTVZA-GY data from Meteor-M N2 satellite. In ITSC-XX: Lake Geneva, Wisconsin, USA, 28 Oct.–3 Nov. 2015. IEEE

Uspensky, A., Asmus, V., Kozlov, A., Kramchaninova, E., Streltsov, A., Chernyavsky, G., Cherny, I. 2017. Absolute calibration of the MTVZA-GY microwave radiometer atmospheric sounding channels. Izvestiya, Atmos. Ocean. Phys. Vol. 53, 1192–1204.

[Discuss the article](#)

External Calibration of MTVZA-GY/ Meteor-M No. 2 Imager Channels

By Leonid Mitnik, Vladimir Kuleshov (*Pacific Oceanological Institute, POI FEB RAS, Vladivostok, Russia*), Grigory Chernyavsky and Igor Cherny (*AO Russian Space System, Moscow, Russia*)

The spacecraft "Meteor-M" No. 2 with the conical scanning microwave imaging/sounding radiometer MTVZA-GY onboard was launched on July 8, 2014 into a sun synchronous orbit at an altitude ≈ 830 km with an inclination of 98.7° . The viewing angle of MTVZA-GY is 53.3° and the incidence angle with respect to the Earth surface is 65° . MTVZA-GY operating frequencies, ν , are located in the transparency windows of the atmosphere at 10.6, 18.7, 23.8, 31.5, 36.5, 42.0, 48.0, and 91.6 GHz, in the oxygen absorption band from 52 to 57 GHz and around the strong water vapor absorption line at 183.31 GHz. The MTVZA-GY imager channels can be used for retrieval of total water vapor content V , total cloud liquid water content Q , sea surface temperature (SST) and wind speed W , land surface temperature (LST) and emissivity $\kappa(\nu)$, as well as to study atmosphere and cryosphere processes, etc. (Barsukov et al., 2016; Chernyavsky et al., 2018; Mitnik et al., 2017; 2018).

On board (internal) and external calibrations were used to transform the MTVZA-GY measured antenna temperatures $T_a(\nu)$ into the brightness temperatures $T_b(\nu)$. Several criteria were developed for selection of the "warm" and "cold" reference areas for external calibration of imager channels. The criteria were determined as a result of T_b s simulation under variations of environmental conditions in the broad

range (Barsukov et al., 2016; Mitnik et al., 2017). The cold ocean zones away from the coast with weak winds, clear sky and low atmospheric water vapor were used as the cold reference areas. These areas can be detected by the joint analysis of the Tah(10), Tah(42) or Tah(91) fields with horizontal (h) polarizations, SST and V charts with the resolution of $1^\circ \times 1^\circ$ available from several sites. The size of these areas should be larger than $5^\circ \times 5^\circ$. They also should have the minimal $T_a(10)$ values and small ($\leq 1K$) $T_a(42)$ variations; SST should be $\leq 10^\circ C$ and $V \leq 3$ kg/m². These areas stand out against the surrounding waters where T_a s are higher due to clouds, winds and increased V values. The tropical Amazon broadleaves rain forests were used as a warm reference target. Several areas with almost uniform $T_a(\nu)$ and sizes $\geq 5^\circ \times 5^\circ$ without signs of the open water (patches and bands of the lower T_a s at $\nu \leq 19$ GHz) were selected. The heavy clouds and rains also manifested themselves by the decrease of T_a s against the surrounding background at $\nu \geq 36$ GHz. (The MTVZA-GY includes complementary new frequencies (42.0 GHz, and 48.0 GHz) for cloud liquid water and oceanographic research) (Mitnik et al., 2017).

The "warm" (Amazon forest) and "cold" (the open ocean just to the north of Antarctica) reference areas can be selected on the same ascending or

descending orbits. In such a case, the time difference between the satellite measurements over warm and cold test areas was less than 30 min.

T_b s over the selected warm and cold calibration areas were computed by numerical integration of the microwave radiative transfer equation (Mitnik and Mitnik, 2003; Mitnik et al., 2017) and served to transfer the MTVZA-GY antenna temperatures into the brightness temperatures. T_b s were also computed for GCOM-W1 AMSR2 channels at frequencies of 10.6, 18.7, 23.8, 36.5 and 89.0 GHz at the incidence angle of 55° . The vertical profiles of atmospheric pressure, temperature and humidity obtained by the nearest radiosonde stations or taken from the reanalysis data, SST as well as the empirical values of forest emissivities were used as the input information.

The long-term stability of MTVZA-GY radiometer in flight was estimated by the statistical analysis of the time series of the daily T_b s measured by the MTVZA-GY and GCOM-W1 AMSR2 and averaged over the selected test areas. The AMSR2 data were used as a reference. Figure 1 shows the time series of the daily averaged brightness temperatures for the period from 1 October 2014 to 30 June 2017 as measured by MTVZA-GY and

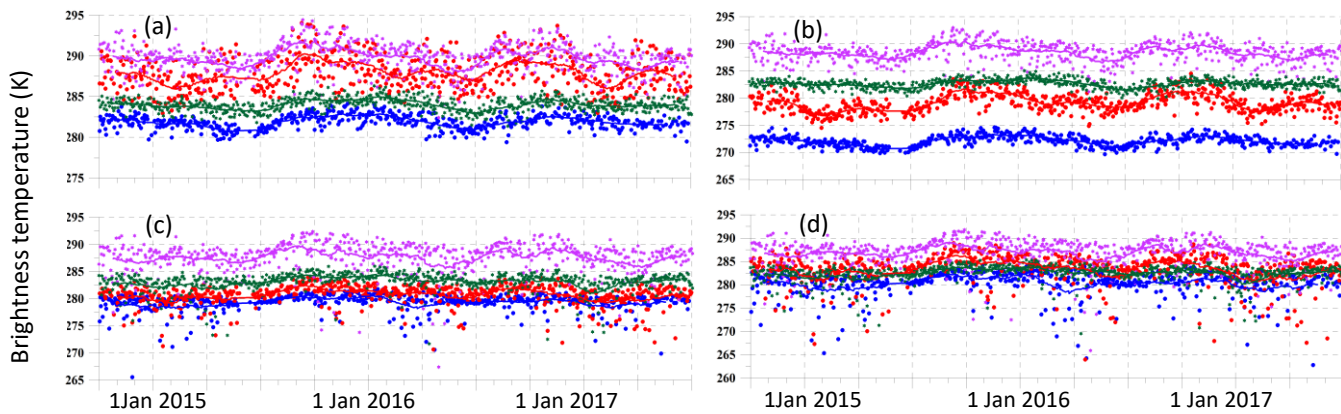


Figure 1. Time series of the brightness temperatures over the test area in the Amazon rain forest ($4^{\circ}27'S$, $56^{\circ}37'W$) at frequencies 10.6 (a), (b) and 36.5 GHz (c), (d) with the vertical (a), (c) and horizontal (b), (d) polarizations. The dots are daily averaged T_b s acquired by MTVZA-GY (blue and red) and AMSR2 (violet and green) at ascending (blue and violet) and descending (red and green) orbits.

AMSR2 radiometers at 10.6 and 36.5 GHz over the Amazon forest reference area with the center at $4^{\circ}27'S$, $56^{\circ}37'W$ (Chernyavsky et al., 2018). The seasonal changes of T_b s are clearly expressed as well as the rain events which are detected due to the decreased T_b s at 36.5 GHz. The time series of the MTVZA-GY and AMSR2 T_b s were also obtained for the test areas in Antarctica near Concordia station and in Greenland near Summit station.

References

- Barsukov, I., Cherniavsky, G., Cherny, I., Mitnik, L., Kuleshov, V., and Mitnik, M. 2016. New Russian meteorological satellite Meteor-M N 2: Sensing of the subsurface, surface and atmospheric characteristics by MTVZA-GY microwave imager/sounder. In Intern. Geosci. Remote Sens. Symp. (IGARSS), IEEE, 5528-5531.
- Cherniavsky, G.M., Mitnik, L.M., Kuleshov, V.P., Mitnik, M.L., and Cherny, I.V. 2018. Microwave sensing of the Ocean, atmosphere and land surface from Meteor-M No. 2 data, Current problems of the Earth Remote Sensing from Space, vol. 15, (in press, in Russian).
- Cherny, I.V., Mitnik, L.M., Mitnik, M.L., Uspensky, A.B., and Streltsov, A.M. 2010. On-orbit calibration of the Meteor-M microwave imager/sounder. In Intern. Geosci. Rem. Sens. Symp. (IGARSS), IEEE, 558–561.
- Mitnik, L., Kuleshov, V., Mitnik, M., Streltsov, A.M., Cherniavsky, and I., Cherny, I. 2017. Microwave scanner sounder MTVZA-GY on new Russian meteorological satellite Meteor-M N 2: modeling, calibration and measurements, IEEE J. Selected Topics Appl. Earth Obs. Remote Sens. Vol. 10. N. 7. P. 3036-3045.
- Mitnik, L.M., Kuleshov, V.P., Mitnik, M.L., and A.V. Baranyuk, 2018. Passive microwave observations of South America and surrounding oceans from Russian Meteor-M No. 2 and Japan GCOM-W1 satellites, Intern. J. Remote Sens. DOI: 10.1080/01431161.2018.1425569.
- Mitnik, L.M., and Mitnik, M.L. 2003. Retrieval of atmospheric and ocean surface parameters from ADEOS-II AMSR data: comparison of errors of global and regional algorithms. Radio Science. Vol. 38, № 4, 8065, doi: 10.1029/2002RS002659.
- Mitnik, L.M., and Mitnik, M.L. 2016. Calibration and validation as prerequisite components of microwave radiometer measurements from Meteor-M No. 2 series satellites, Current problems of the Earth Remote Sensing from Space, vol. 13, No. 1, pp. 95-104 (in Russian).

[Discuss the article](#)

Radiometric inter-calibration of MSU-MR shortwave channels on-board Meteor-M No. 2 relative to AVHRR on-board Metop-A

By A. Filei, A. Rublev (State Research Center for Space Hydrometeorology "Planeta", Roshydromet) and A. Zaitsev (Joint Stock Company Russian Space Systems)

The Meteor-M No. 2 is a polar-orbiting meteorological satellite (Asmus et al., 2014). It was launched on July 8, 2014 and is located at an altitude of 827 km with a 9:10AM LECT. The MSU-MR (Multi-Channel Scanning Unit of Middle Resolution) scanner on-board Meteor-M is a 6-channel instrument. Three shortwave channels with central wavelengths at 0.6, 0.83, 1.7 microns

have onboard calibration in space. The spatial resolution is approximately 1 km. The swath width is about 2800 km. In the paper, we present the results of radiometric inter-calibration of MSU-MR shortwave channels relative to radiometer AVHRR/3 (Advanced Very High Resolution Radiometer) on-board Metop-A (9:30 AM LECT). The AVHRR/Metop-A data were used as a

reference because this instrument regularly participate inter-calibrations and has the channel spectral functions similar to MSU-MR.

Figure 1 shows a comparison of the normalized spectral response functions (SRF) of the first three shortwave channels (ch.1, ch.2, ch.3) of MSU-MR and AVHRR instruments.

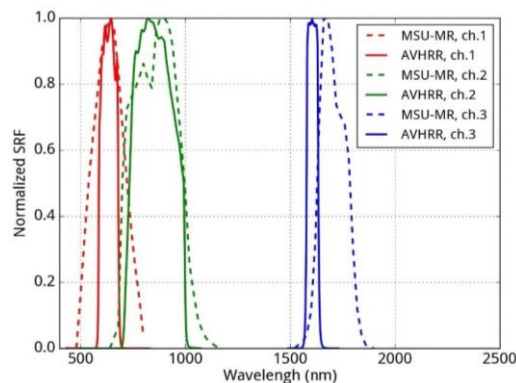


Figure 1. Normalized spectral response functions of the first three shortwave channels

Site Location	k ₁	Std.dev	k ₂	Std.dev	k ₃	Std.dev
Libya 1	1.102	0.022	1.189	0.030	1.081	0.023
Libya 2	1.074	0.010	1.196	0.010	1.125	0.014
Sudan 1	1.094	0.008	1.205	0.010	1.104	0.008
Algeria 3	1.096	0.012	1.179	0.012	1.118	0.011
Niger 2	1.099	0.009	1.208	0.009	1.103	0.009
Egypt 1	1.063	0.016	1.191	0.012	1.120	0.012
The average	1.089	0.004	1.198	0.004	1.110	0.004
SBAF	0.981	-	1.010	-	1.053	-
Calibration coefficients	1.111	0.004	1.186	0.004	1.054	0.004

Table 1. Coefficients of proportionality between MSU-MR & AVHRR channels for six sites.

The analysis of Figure 1 shows the SRF differences for channels of both satellite instruments. To account for these differences, a regression relationship between corresponding channels of the two satellite instruments has been calculated. Under similar observation angles and positions of the Sun, we have identified directly proportional relationships between reflectance coefficients

measured by both satellites in all shortwave channels. The calculated spectral band adjustment factors (SBAF) (from AVHRR to MSU-MR) are equal to 0.981; 1.010; 1.053 respectively for each pair of channels. Spectral band adjustment factors are calculated as follows:

$$\text{SBAF} = \frac{L_{\text{AVHRR}}}{L_{\text{MSU-MR}}} \quad (1)$$

where L is pseudo-scaled radiances.

The simulation of the pseudo-scaled radiances values was carried out by the Monte Carlo method. Pseudo scaled radiances modeling was carried out for each MSU-MR and AVHRR channel for the sand surface.

To avoid errors associated with discrepancies in observation angles and positions of the Sun, cloudless cases were selected when the orbits of the two satellites coincided in flight time

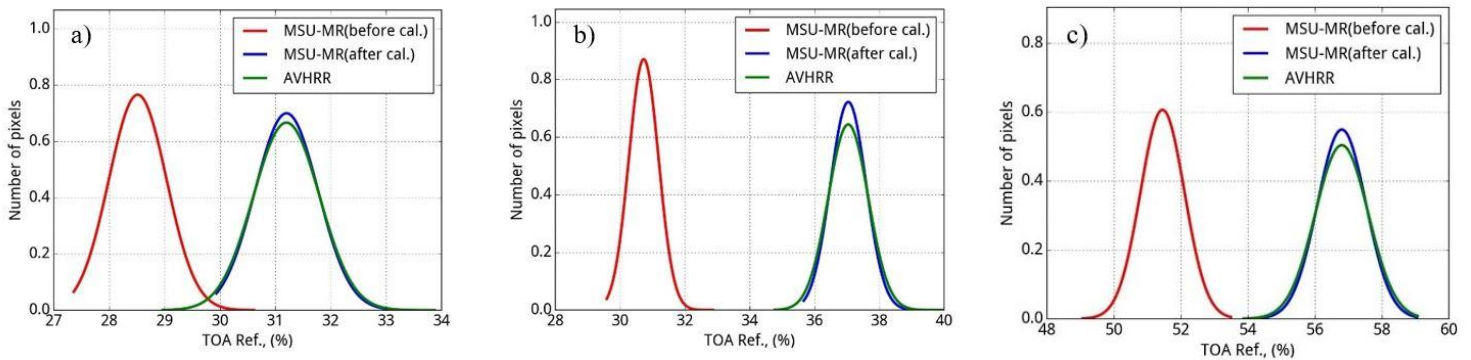


Figure 2. The normalized distribution number of pixels of the TOA reflectance for the Sudan1 Site: a) the first channels; b) the second channels; c) the third channels.

as well as in the angle of observation over the given study region. According to Datla et al., 2011, with an agreement angle within 2° , the difference in measurements can vary from 0.2 to 0.3%.

We used six test sites within the framework of the CEOS (https://calval.cr.usgs.gov/rst-resources/sites_catalog/radiometric-sites/maps/sites_catalog_africa/) for comparison. These sites are presented in Table 1. The satellites cross the equator with a difference of 15 minutes, and the viewing angles of the AVHRR and MSU-MR lay within 3° . The spatial distance of the collocated AVHRR & MSU-MR pixels scanned at similar angles was 1 km. The maximum viewing satellite angle when comparing the top of atmosphere (TOA) reflectance values did not exceed 35° .

The inter-calibration method is based on a comparison of the reflectance at the TOA of two instruments in the visible and near infrared wavelengths (Filei et.al., 2016). The purpose of the inter-calibration is to find the empirical calibration constants k_N for the MSU-MR channels, which would provide the minimal deviation from the TOA reflectance values obtained from the

AVHRR channels. TOA reflectance values from the AVHRR channels were calculated from the radiances, which were received from FRAC (Full Resolution Area Coverage) AVHRR data (<https://www.class.ngdc.noaa.gov/saa/products/welcome>). The TOA reflectance R is derived from AVHRR and MSU-MR radiance and solar flux at the TOA as follows:

$$R = \frac{\pi \cdot L \cdot d^2}{F \cdot \cos(SZA)} \quad (2)$$

where L is a measured radiance; F is an effective flux calculated by convolving the solar spectral irradiation with the instrument SRF within the channel band; d is the Earth-Sun distance factor in astronomical unit; SZA is the Sun zenith angle.

The ratio connecting the TOA reflectance of the AVHRR (R_{AVHRR}) and the MSU-MR (R_{MSU-MR}) can be written in the form

$$R_{AVHRR} = k_N \cdot R_{MSU-MR} \quad (3)$$

where k_N is the coefficient, N is channel number.

Thus, the average proportionality coefficients shown in Table 1 were computed for each pair of instrument channels over all six test sites. For each test site, more than 2000 matched TOA reflectance pairs were used. The time

period of the data used was 18-20 April, 2017. The calibration coefficients, determined as the ratio between obtained k_N and SBAF, are shown in the lowest row of the table. For example, the MSU-MR reflectance values for the Sudan1 site are shown in Figure 2 before calibration (red color) and after calibration (blue color) with using gain coefficient. The AVHRR reflectance values are also presented in the graphs (green color).

As can be seen from the figure, using the coefficients k_N , it is possible to achieve better alignment of the reflectance values over all three channels of AVHRR and MSU-MR. After performing the intercalibration, it is possible to join the data of AVHRR & MSU-MR to calculate various complex indices characterizing the state of the underlying surface.

For example, as is shown in (Filei et al., 2016), after intercalibration the humidity index maps of the soils calculated according to both instruments data almost completely coincide.

References

Asmus V.V., Zagrebaev L.A., Makridenko O.E., Milekhin O.E., Solov'yev V.I., Uspensky A.B., Frolov A.V., Khaylov M.N., 2014, The system of polar-orbiting meteorological satellite Meteor-M series, *Meteorologiya i gidrologiya*, No. 12, 5-16

Datla R.U., Rice J. P., Lykke K.R., Johnson B. C., 2011, Best Practice

Guidelines for Pre-Launch Characterization and Calibration of Instruments for Passive Optical Remote Sensing, *Journal of research of the National Institute of Standards and Technology*, Vol. 116, No. 2, 621-646, DOI: 10.6028/jres.116.009

Filei A.A., Rublev A.N., Zaitsev A.A., 2016, Radiometric cross-calibration of shortwave channels of multi-channel scanning unit on board Meteor-M no. 2

relative to spectroradiometer AVHRR on board Metop-A. *Sovremennye problemy distantsionnogo zondirovaniya Zemli iz kosmosa*, Vol. 13, No. 6, 251-263, (in Russian), DOI: 10.21046/2070-7401-2016-13-6-251-263

[Discuss the article](#)

Radiometric inter-calibration between MSU-GS and VIIRS shortwave channels

By A. Filei, A. Rublev, Yu. Kiseleva (State Research Center for Space Hydrometeorology "Planeta", Roshydromet) and A. Zaitsev (Joint Stock Company "Russian Space Systems")

Elektro-L No. 2 is the second in the new-generation of Russian meteorological satellites operated from the geostationary orbit. It was launched on December 11, 2015 and positioned at 76° east longitude. The primary instrument onboard the Elektro-L satellite is the MSU-GS ten-channel scanner that is capable of obtaining the Earth's images every 30 minutes. The visible and infrared channels of the sensor have nadir resolutions of one and four kilometers, respectively. For support in emergency situations, the scanner is capable of taking snapshots as fast as one in 10-15 minutes (<http://www.russianspaceweb.com/elektro.html>).

MSU-GS covers three shortwave channels with central wavelengths of 0.57, 0.72 and 0.86 microns. In the paper, we present the results of radiometric inter-calibration of these channels relative to the VIIRS radiometer on-board Suomi NPP. VIIRS was used as a reference because

this instrument regularly participates in inter-calibrations and has the channel spectral functions similar to MSU-GS with central wavelengths of 0.555(M04), 0.672(M05), 0.865(M07) microns. Figure 1 shows a comparison of the normalized spectral response functions (SRF) of the first three

shortwave channels of MSU-GS and VIIRS.

The inter-calibration method is based on a comparison of reflectance at the top of atmosphere (TOA) measured by both instruments in the corresponding channels. The purpose of the inter-calibration is to find the empirical calibration constants k_N providing

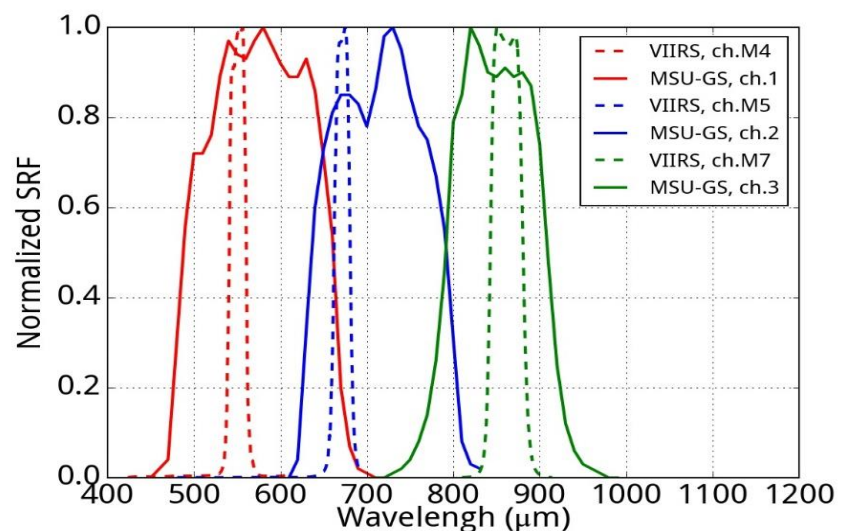


Figure 1. Normalized spectral response functions of the three shortwave channels of MSU-GS and VIIRS instruments.

Table 1. Coefficients of proportionality between MSU-MR & AVHRR channels for six sites

Month	k ₁	Std error*	k ₂	Std error	k ₃	Std error	Number of cases
April	0.959	0.021	1.091	0.038	1.096	0.031	384
May	0.995	0.009	1.082	0.010	1.126	0.012	383
June	0.980	0.095	1.049	0.091	1.076	0.076	227
July	0.978	0.036	1.052	0.040	1.088	0.035	651
August	0.974	0.118	1.066	0.120	1.086	0.118	116
September	0.987	0.035	1.052	0.037	1.116	0.030	554
Weighted mean	0.989	0.008	1.079	0.009	1.118	0.010	2315

*Std error – standard regression error

minimal discrepancy between TOA reflectance measured by MSU-GS and VIIRS channels. For comparison, we used measurements above deep convective clouds (DCCs) over the Indian Ocean. The DCC technique is an alternative variant of the target calibration approach. The benefits of its use for inter-calibration in comparison with the bright land targets lies in the fact that DCCs are located in the upper troposphere; therefore, the decreasing effect of water vapor and aerosol on the value of reflectance equals epsilon squared (Doelling et.al., 2011, Sterckx et.al.,2016).

The pixels in the M15 VIIRS band (11- μ m) with brightness temperature of less than 205°K were selected for inter-calibration. The DCCs pixel are confined to $\pm 20^\circ$ North/South and East/West of Elektro-L No. 2 subsatellite point. The maximum zenith angle from pixels to Suomi NPP or Elektro-L satellites did not exceed 20 degrees, and the difference between the angles was within 5 degrees. The time intervals between the measurements of both satellites were less than 15 minutes. The data used in the inter-calibration were obtained between April and September 2017.

Although DCC reflectance have no significant variation in the visible spectrum, the differences in spectral response functions (SRF) between the reference and monitoring sensor (Figure 1) can introduce a serious error to inter-calibration (Doelling et.al., 2011). In order to account for this difference, a spectral band adjustment factor (SBAF) for the corresponding channels of the two satellite instruments has been calculated:

$$SBAF = \frac{L_{VIIRS}}{L_{MSU-GS}} \quad ..(1)$$

where L - simulated TOA reflectance. The simulation of the TOA reflectance was carried out by using LibRadtran (<http://www.libradtran.org>) with the ice particle model for DCC (Baum et.al., 2005a). More details on the TOA reflectance simulation for DCC can be found in (Sohn et.al., 2009). As a result, the calculated SBAF for MSU-GS and VIIRS approximately equaled 1.0 for each pair of channels. Therefore, the compared TOA reflectances must be equal. The TOA reflectance values from the VIIRS channels were taken from VIIRS SDRs (Sensor Data Records) (<https://www.class.ngdc.noaa.gov/saa/products/welcome>). The TOA

reflectance R derived from MSU-GS radiance and solar flux at the TOA was as follows:

$$R = \frac{\pi \cdot L \cdot d^2}{F \cdot \cos(SZA)} \quad ..(2)$$

where L - measured radiance; F - effective flux calculated by convolving the solar spectral irradiation with the instrument's SRF within the channel band; d - the Earth–Sun distance factor in astronomical unit; SZA - the Sun's zenith angle.

The ratio connecting the TOA reflectance as measured by VIIRS (R_{VIIRS}) and MSU-GS (R_{MSU-GS}) can be described by the following equation:

$$R_{VIIRS} = k_N \cdot R_{MSU-GS} \quad ..(3)$$

where k_N - calibration constants, n - channel number.

Thus, the weighted mean regression coefficients shown in Table 1 were computed for each pair of MSU-GS and VIIRS channels over five months. Figure 2 shows examples of the TOA reflectance regression between the channel pairs of both sensors for each month. Since the calculated SBAF between MSU-GS and VIIRS equaled approximately 1.0 for each pair of channels, the average regression coefficients (Table 1), in fact, show the

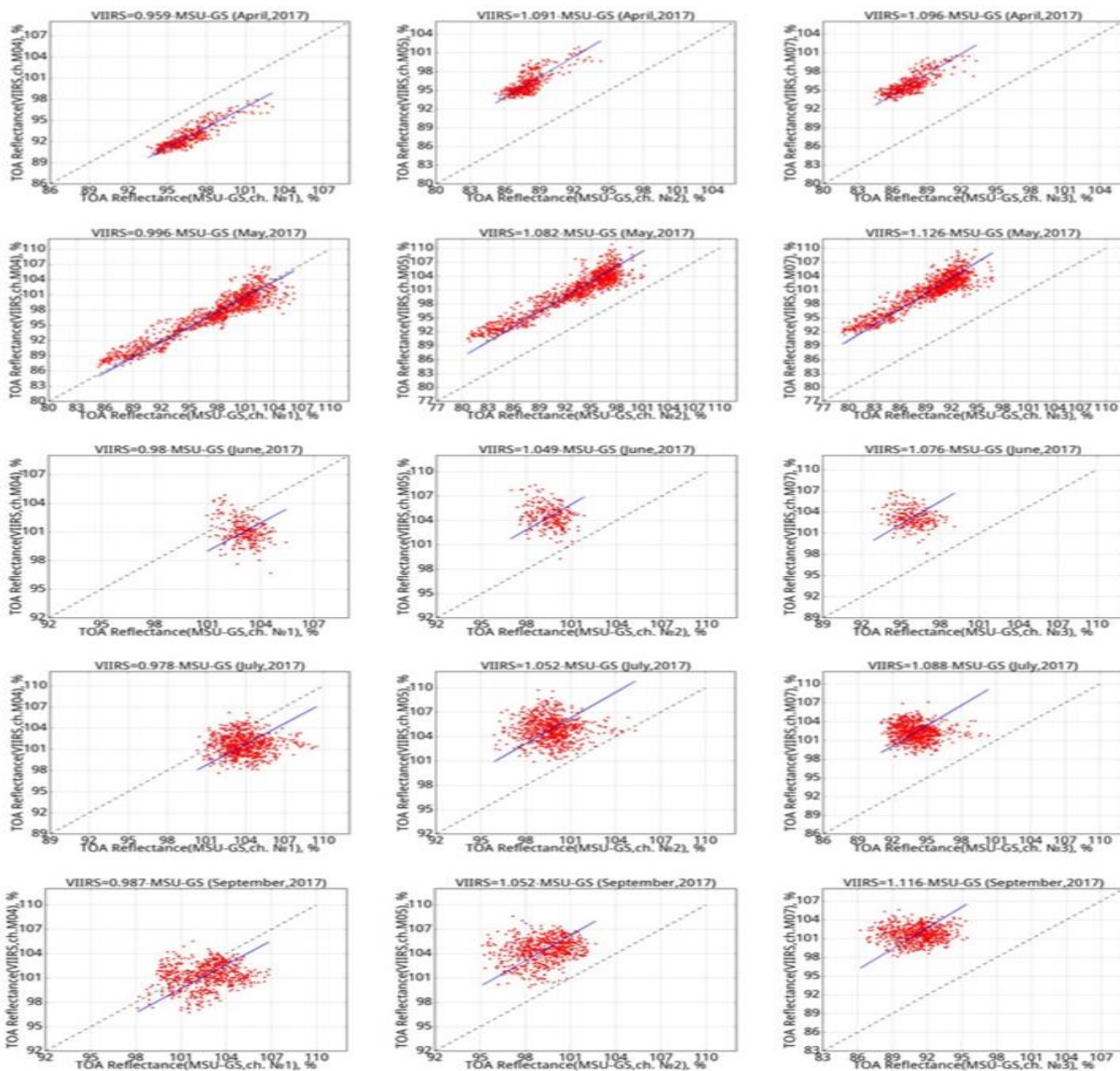


Figure 2. Regression of TOA reflectance for three pairs (MSU-GS & VIIRS) of shortwave channels

true differences between the TOA reflectance values of the respective channel pairs of VIIRS and MSU-GS sensors. The first MSU-GS channel demonstrates good agreement with M04 VIIRS channel (the difference is only about 2%), the differences for the second and third MSU-GS - VIIRS channel pair are more significant; they amount to 8% and 12%, respectively.

References

Baum B.A., Yang P., Heymsfield A.J., Platnick S., King M.D., Hu Y-X.,

Bedka S.T. Bulk scattering models for the remote sensing of ice clouds. Part II: Narrowband models, *Journal of Applied Meteorology and Climatology*, 2005a, Vol. 44, pp.1896-1911, DOI:10.1175/JAM2309.1

Doelling, D.R., Morstad D.L., Bhatt R., Scarino B. Algorithm Theoretical Basis Document (ATBD) for Deep Convective Cloud (DCC) Technique of Calibrating GEO Sensors with Aqua-MODIS for GSICS, GSICS, 2011, 11 p.
Sohn B.-J., Ham S.-H., Yang P.

Possibility of the visible-channel calibration using deep convective clouds overshooting the TTL, *Journal of Applied Meteorology and Climatology*, 2009, Vol. 48, pp. 2271-2283, DOI: 10.1175/2009JAMC2197.1
Sterckx S., Adriaensen S., Dierckx W., Bouvet M. In-Orbit Radiometric Calibration and Stability Monitoring of the PROBA-V Instrument, *Remote Sensing*, 2016, Vol. 8(7), 21 p. DOI:10.3390/rs8070546.

[Discuss the article](#)

News in this Quarter

Highlights on 2018 Annual GRWG/GDWG Meeting

by M. Bali (UMD), L. Flynn (NOAA), P. Zhang (CMA), S. Hu (CMA), T. Stone (USGS), D. Doelling (NASA), R. Ferraro (NOAA), T. Hewison (EUMETSAT), D. Kim (KMA) and M. Takahashi (JMA)

This year's meeting of the GRWG and GDWG was organized by the China Meteorological Administration (CMA) and hosted by Shanghai Institute of Technical Physics (SITP) in Shanghai, China on 19 - 23 March 2018. Members from ESA, IMD, JMA, ISRO, NIST, KIOST, JAXA, NASA, NOAA, CMA, CAS, EWU, SITP, CNES, KMA, USGS, EUMETSAT, and University of Leicester attended the meeting.

After impressive welcoming speeches by Peng Zhang (previous GSICS EP Chair) and Lei Ding (Deputy Director of SITP), Dohyeong Kim (GRWG Chair) introduced the Mini Conference, which covered topics vital to GSICS in the near future. CMA and SITP highlighted the current and future pre-launch and post launch calibration work done for a wide range of instruments manifested on platforms that they have launched or are building. Peng Zhang began the session with a progress report on FY-3D and FY-4 series which was followed by a topic on SI-traceable targets for hyperspectral FTIR instrument. Qiang Guo informed members about the status of commissioning of the FY-4A and Zhangdong Yang detailed the post-launch test progress of FY-3D.

Mitch Goldberg (GSICS EP Chair), Feng Jiang, Yanmeng Bi and Deku Yin covered topics on NOAA-20 SDR maturity, solar band SI traceable instrument, Tansat/ACGS post launch calibration and TG-2 Multi Angle Polarization, respectively.

The Mini Conference was followed by the Plenary Meeting chaired by Dohyeong Kim (KMA).



Participants of the GSICS Annual Meeting 2018, Shanghai, China

In the first part of the Plenary session, representatives from CMA, ESA, IMD, EUMETSAT, JAXA, JMA, KMA, ISRO, NIST, NOAA and USGS presented their agency reports. The plenary continued the next day with reports from the chairs of the GCC, GRWG and GDWG.

The GCC report was given by L. Flynn (GCC Director). In the past year, GCC has published four GSICS Newsletters and supported a GSICS session in the AOMSUC-8. Seven new products (six Himawari versus IASI-A/-B cross-calibration products and one MSG-4 versus IASI-A bias correction product) were promoted into the GSICS fold.

Following the plenary there were four breakout sessions each dedicated to one of the subgroups: UV, IR, MW or VIS/NIR.

UV Sub-Group Session Summary

The UV session was a very informative mix of talks on ground-based calibration of cutting-edge instruments under development, in-orbit calibration and characterization of operational sensors, and methods for comparing and monitoring long-term records. Chinese Academy of Science and CMA researchers (Yongmei Wang, Guanyu Lin, Houmao Wang and Yuan Li) provided results of SNO comparisons of SBUS and TOU instruments on the FY-3 series of satellites with the Metop GOME-2 and NOAA OMPS instrument measurements. Presentation on next generation CMA UV instruments (the High-Resolution TOU), the follow-ons to the Limb Imaging Spectrometer (LIS) and Annular UV Imager (AUI) flown on the Tiangong-2 Space Laboratory initiated interesting discussions.

L. Flynn gave a comparison of the performance of the recently launched NOAA-20 OMPS and that of the S-NPP OMPS. On the UV Solar Project, Mina Kang of EWU provided the results of comparisons of UV spectral using measurements from the recently launched Sentinel 5P TropOMI instrument. The final talk of the session was an update on NOAA and (some NASA) activities related to three of the UV projects.

IR Sub-Group Session Summary

The IR session started with an update on the progress of GEO-LEO IR products. The session then reviewed the [spectral gap-filling](#) method proposed by Xu Hui to compensate the CrIS large spectral gap, an [evolved approach](#) within the GSICS framework presented by Tim Trent, and a new improved [collocation](#) algorithm developed by Likun Wang.

The session went on to accept CrIS as a GSICS reference. The impact of change in the IASI-B processing in August 2017 was also analyzed, which revealed small but significant differences - so EUMETSAT were encouraged to indefinitely delay changing IASI-A. The plans to write GSICS IR Reference Uncertainty and Traceability Report ("IRRefUTable") were also discussed, targeting first draft later in 2018. The group agreed working together on the white paper to document the best practice of IR hyperspectral sounding processing. Coordination with the SCOPE-CM IOGEO project on the GEO-ring test dataset was also recommended. The meeting was ended by electing Likun Wang as a new IR subgroup chair and with thanks for Tim Hewison for his great contributions.

MW Subgroup Session

The Microwave breakout session discussed topics such as inter-calibration, pre-launch characterization

and "best practices." Hosts CMA and SITP utilized the session to showcase the strides made in China in Microwave sensor calibration and the breakout session for their operational imagers and sounders on the FY3 satellite series.

The session also proved to be a ground to discuss best practices for GSICS Microwave inter-sensor calibration. The plan to develop a GEO MW sounder was presented by Hao Liu (NSSC) following initiated discussions on monitoring this GEO instrument with LEO reference records similar to that done in the IR. NOAA and CMA also discussed the use of GPSRO as a calibration reference for certain MW channels (e.g., oxygen bands)

VIS/NIR Sub Group Session Summary

The VIS/NIR GRWG was divided into two sessions. The lunar session was held in the morning and the Earth viewed calibration activities during the afternoon.

The lunar session started with a report prepared by EUMETSAT on the outcomes of the 2nd GSICS/CEOS-IVOS Lunar Calibration Workshop, which was held at Xi'an, China in November, 2017. The workshop covered many diverse lunar calibration topics, including data processing for lunar irradiance measurements, development of a lunar inter-calibration strategy, and alternative uses of Moon observations such as Modulation Transfer Function (MTF). Tom Stone reported on the GIRO benchmark, which was developed by EUMETSAT to validate the GIRO lunar reference against the USGS ROLO model. Initial validation testing has begun at USGS. In the afternoon session that focused on Earth View, CMA provided Updates on their FY-3 VIRR and MERSI imager performance, calibration and validation, as well as the TANSAT-CAPI imager

performance, calibration and validation were discussed.

The breakout session noted that the inflight performance of the NOAA-20 or JPSS-1 VIIRS is as good as SNPP-VIIRS and that the Terra-MODIS, Aqua-MODIS, SNPP-VIIRS, and NOAA-20 VIIRS can act as series of in-orbit references that can be used to transfer to a future absolute calibration reference back in time to the year 2000.

The VIS/NIR group planned to design a Rayleigh scattering calibration technique based on best practices as a GSICS endorsed calibration technique. It also decided to extend the Deep Convective Cloud (DCC) approach into the NIR wavelengths.

GSICS Data Working Group (GDWG) Session Summary

In the Data Working Group sessions, 18 topics such as reviewing GSICS member agencies' websites, mirroring GSICS Collaboration Servers, use of GitHub for GSICS activities, updates of GSICS action tracking tool, future migration plan of GSICS wiki and GDWG Terms of Reference (ToR) updates were discussed. Some of the topics are stated here.

Updates on the GSICS collaboration server were discussed in the breakout session. Currently CMA, EUMETSAT and NOAA are the hosting the collaboration servers. In 2017, ISRO also launched their own GSICS server, and the updates of the server configuration for 4th Collaboration Servers is underway in collaboration with EUMETSAT.

The breakout session reviewed GRWG requirements on extending the functionality of GSICS Plotting Tool to plot the VNIR products, and it will be implemented by EUMETSAT. CMA and NOAA presented their Instrument Performance Monitoring systems The Integrated Calibration and

Validation System (ICVS) at STAR and the FY Satellite monitoring system are similar. They are powerful tools to monitor instruments performance and display it on World Wide Web.

Cross cutting discussions

In response to actions in GSICS-EP-18 (June 2017, Jeju), the groups discussed two cross cutting topics. The first one

was the, state of the observing system calibration reports for each GSICS member agency and the second topic was the preparation of specifications and methodologies for operational instrument performance monitoring system. GRWG Chair introduced several existing systems such as ICVS and expected minimum requirements were discussed. In order to build

consensus on these topics, members recommended to organize workshops on s Best practice of IR hyperspectral sounding processing, Traceable Hyperspectral Reference Workshop, Potential workshop on best practices for pre-launch instrument characterization.

This article has been condensed from a summary of the Annual Meeting prepared by co-authors and is available with the GCC



GOES Calibration Web Site

by R. Iacovazzi, Jr. (NOAA GPRC)

The Advanced Baseline Imager (ABI) is the primary payload for NOAA's Geostationary Operational Environmental Satellite R-series (GOES-R). The ABI incorporates many new technologies to meet the more demanding NOAA Consolidated Observing User Requirement List (COURL) - established by NOAA program leaders and subject matter experts - compared to that of the previous GOES N-Series. The first of this new generation GOES was launched on November 19, 2016, and named GOES-16 when it reached orbit on November 29, 2016. There is great interest within the GOES-R Program and the user community, as well as amongst international partners, to determine whether ABI meets performance expectations, and to compare its performance to the current GOES N-series Imager. The NOAA GOES Calibration web site (<https://www.star.nesdis.noaa.gov/GOESCal/index.php>) is a critical tool that helps to enable these activities.

The GOES Calibration web site is a one-stop shop for near- and long-term monitoring of GOES instrument radiometric calibration, thermal

character and stability, as well as GOES-R ABI L1b product radiometric, image navigation and registration, and spectral performance. The foundation of the site is a plethora of comprehensive instrument and L1b product quality data sets that are accessible in near-real time exclusively to GOES calibration specialists with NOAA local-area network access. The primary GOES-16 ABI data sources include:

- Instrument calibration data and engineering telemetry
- Level-1b (L1b) radiances
- Image Navigation and Registration (INR) offsets with respect to landmark data
- Observed minus Community Radiative Transfer Model (CRTM) simulated infrared radiances
- Statistics of GOES-R instrument measurement biases with respect to measurements from similar instruments on other polar and geostationary satellite instruments
- Vicarious calibration trending parameters associated with

lunar, desert, and deep convective cloud methodologies

For operational heritage GOES Imager and Sounder, engineering telemetry are the predominant data sets.

These comprehensive data sets support deep-dive calibration analysis, and aid anomaly resolution and long term monitoring performed by the GOES calibration specialists. They also support the generation of the many plots and graphs that are posted on the GOES Calibration web site. The content served by the web site provides GOES calibration specialists, worldwide satellite operators, science community members and data users on-line access to instrument and L1b product quality information and graphics to foster instrument and L1b product integrity knowledge and anomaly detection.

On-orbit validation, and data integrity, of GOES L1b products is important through all phases of post-launch instrument life to ensure that these measurements meet instrument specifications and data user needs. The GOES Calibration web site provides

insight into this with analysis products that rely heavily on tested and peer-reviewed on-orbit calibration methodologies, many of which have matured as a result of GSICS collaboration. In progressing towards

the GEOSS concept of improving weather and climate products to benefit society, initiatives such as the Global Space-based Inter-calibration System (GSICS) are designed to support the measurement synergy amongst LEO

and GEO satellite instruments. These initiatives create opportunities to use global-community developed satellite inter-calibration methods to evaluate GOES instruments, which is reflected in the GOES Calibration web site.

[Discuss the article](#)

Announcements

Call for papers for 2nd Workshop of the CGMS International Cloud Working Group (ICWG)

by *Andy Heidinger (NOAA) and Rob Roebeling (EUMETSAT)*

The organizing committee cordially invites scientists and researchers from around the world, who work in cloud physics and/or the retrieval of cloud parameters from satellite observations, to participate in the 2nd Workshop of the ICWG. The 2nd Workshop of the CGMS International Cloud Working Group (ICWG-2) will take place from 29 October 2018 through 2 November 2018 in Madison, Wisconsin, USA. This workshop will be organized by the University of Madison, Wisconsin, and is co-sponsored by EUMETSAT and NOAA. The main topics of ICWG-2 are:

- Algorithms
- Assessments
- Climate Applications
- Weather Applications

The ICWG-2 participants are encouraged to contribute to one (or more) of these Topical Groups. The topics and the leads of these Topical Groups are listed in the announcement. Please contact the leads of the Topical Groups and discuss with them how you would like to contribute. For further information on the workshop, please visit the announcement page from a link at

<http://www.icare.univ-lille1.fr/crew/index.php/Meetings>

Sentinel-3B Mission launched

by Tim Hewison and Alessandro Burini (EUMETSAT)

Sentinel-3B was launched on 25 April 2018 at 17:57 GMT from Plesetsk Cosmodrome in Northern Russia; after 1:32 hrs the telemetry signal has been correctly acquired and LEOP operations started.

The successful launch of Sentinel-3B represents the full deployment of the two-satellite Sentinel-3 mission. During the commissioning phase, it is foreseen to fly the platform in a tandem configuration with Sentinel-3A, delayed by 30 seconds. This complex configuration follows a one-month drift period, where the B platform will be slowly drifted in the “tandem” position, which will be maintained for almost four months to allow the cross-calibration of the A and B platform.

Sentinel-3B delivered its first image on 7 May acquired by OLCI, the first instrument to be switched on. OLCI is currently behaving nominally and

preliminary results over vicarious calibration targets (e.g. desert targets) show good agreement with MERIS and small differences with OLCI-A. More interesting results will come when the platforms will be in the tandem configuration.

After OLCI, SLSTR was the second instrument to be switched on. SLSTR is fully nominal and producing visible data, the black bodies were activated on 9 May and tests to heat up the devices have been carried out. The TIR channels will be the last channels to be activated. First inter-calibration tests for SLSTR visible channels vs OLCI-A showed significant differences; data have been processed with the pre-flight calibration coefficients and better results are expected once measurements from the VISCAL device will be acquired. From the first week of June, the tandem phase will start as planned



Image above shows Sentinel-3b being launched

and the Sentinel-3 constellation will be operated in tandem mode until mid-September. The Commissioning phase is planned to be concluded for mid-November 2018.

[Discuss the article](#)

GSICS-Related Publications

- Chen, R., F. Alquaied, and W.L. Jones. 2017. ‘Assessing Radiometric Stability of the 17-Plus-Year TRMM Microwave Imager 1B11 Version-8 (GPM05) Brightness Temperature Product’. *Climate* 5 (4). <https://doi.org/10.3390/cli5040092>.
- Chen, S., N. Xu, T. Dai, X. Zhou, H. Lü, and Y. Cheng. 2018. ‘Sensitivity of Intercalibration Uncertainty on Spectral Sampling of Space-Based Radiance Standard’. *Guangxue Xuebao/Acta Optica Sinica* 38(1). <https://doi.org/10.3788/AOS201838.0128004>.
- Chu, M., J. Sun, and M. Wang, 2018: Performance Evaluation of On-Orbit Calibration of SNPP VIIRS Reflective Solar Bands via Intersensor Comparison with Aqua MODIS. *J. Atmos. Oceanic Technol.*, **35**, 385–403, <https://doi.org/10.1175/JTECH-D-17-0008.1>
- Chang, T., G. Keller, and X.J. Xiong. 2017. ‘Bridging the Thermal Band Comparison between LEO-LEO Sensors and between GEO-GEO Sensors’. In *Proceedings of SPIE - The International Society for Optical Engineering*. Vol.10402. <https://doi.org/10.1117/12.2272794>
- Gierens, K., Eleftheratos, K., and Sausen, R.: Intercalibration between HIRS/2 and HIRS/3 channel 12 based on physical considerations, *Atmos. Meas. Tech.*, 11, 939-948, doi: [10.5194/amt-11-939-2018](https://doi.org/10.5194/amt-11-939-2018), 2018.
- Guo, Qiang, Xuan Feng, Changjun Yang, and Boyang Chen. 2018. ‘Improved Spatial Collocation and Parallax Correction Approaches for Calibration Accuracy Validation of Thermal Emissive Band on Geostationary Platform’. *Ieee Transactions on Geoscience and Remote Sensing* 56 (5): 2647–63. <https://doi.org/10.1109/TGRS.2017.2778744>

Qin, Y., and T.R. McVicar. 2018. 'Spectral Band Unification and Inter-Calibration of Himawari AHI with MODIS and VIIRS: Constructing Virtual Dual-View Remote Sensors from Geostationary and Low-Earth-Orbiting Sensors'. *Remote Sensing of Environment* 209: 540–50. <https://doi.org/10.1016/j.rse.2018.02.063>.

Submitting Articles to GSICS Quarterly Newsletter:

The GSICS Quarterly Press Crew is looking for short articles (~800 to 900 words with one or two key, simple illustrations), especially related to calibration / validation capabilities and how they have been used to positively impact weather and climate products. Unsolicited articles may be submitted for consideration anytime, and if accepted, will be published in the next available newsletter issue after approval/editing. Please send articles to manik.bali@noaa.gov.

With Help from our friends:

The GSICS Quarterly Editor would like to thank Alexey Rublev (ROSHYDROMET), Tim Hewison (EUMETSAT) and Lawrence E. Flynn (NOAA) for reviewing articles in this issue.

GSICS Newsletter Editorial Board

Manik Bali, Editor
Lawrence E. Flynn, Reviewer
Lori K. Brown, Tech Support
Fangfang Yu, US Correspondent.
Tim Hewison, European Correspondent
Yuan Li, Asian Correspondent

Published By

GSICS Coordination Center
NOAA/NESDIS/STAR NOAA
Center for Weather and Climate Prediction,
5830 University Research Court
College Park, MD 20740, USA

Disclaimer

The scientific results and conclusions, as well as any views or opinions expressed herein, are those of the authors and do not necessarily reflect the views of NOAA or the Department of Commerce or other GSICS member agencies.